Extended method of moments for deterministic analysis of stochastic multistable neurodynamical systems

Gustavo Deco* and Daniel Martí
Computational Neuroscience Group, Universitat Pompeu Fabra, Passeig de Circumval·lació, 8, 08003 Barcelona, Spain
(Received 27 November 2006; published 28 March 2007)

The analysis of transitions in stochastic neurodynamical systems is essential to understand the computational principles that underlie those perceptual and cognitive processes involving multistable phenomena, like decision making and bistable perception. To investigate the role of noise in a multistable neurodynamical system described by coupled differential equations, one usually considers numerical simulations, which are time consuming because of the need for sufficiently many trials to capture the statistics of the influence of the fluctuations on that system. An alternative analytical approach involves the derivation of deterministic differential equations for the moments of the distribution of the activity of the neuronal populations. However, the application of the method of moments is restricted by the assumption that the distribution of the state variables of the system takes on a unimodal Gaussian shape. We extend in this paper the classical moments method to the case of bimodal distribution of the state variables, such that a reduced system of deterministic coupled differential equations can be derived for the desired regime of multistability.

DOI: 10.1103/PhysRevE.75.031913 PACS number(s): 87.18.Sn, 05.10.−a, 84.35.+i, 87.19.La

I. INTRODUCTION

Over the course of recent decades, neurophysiological and psychological studies have started to shed light on a large variety of brain functions. Deeper insight into the neural mechanisms underlying many brain functions can only be gained by understanding the basic computational principles behind them. The theory of stochastic dynamical systems offers a useful framework for the investigation of the neural computation involved in perception, cognition, and behavior [1,2]. Stochastic transitions occur in cognitive processes like decision making [3–5], and in perceptual processes like multistable perception [6]. For example, bistable visual phenomena arise when the stimuli presented afford at least two distinct possible interpretations of the same unchanging physical retinal image. Typical examples include the Necker cube, Rubin's face vase, binocular rivalry, and bistable apparent motion [7,8]. Single cell recordings have revealed that only a small proportion of neurons in the low-level visual cortical areas (V1 and V2) are modulated according the perceptual alternation, whereas in high-level visual cortical areas (V4, MT, MST, IT, STS) a high proportion of the neurons vary their activity according to the perceptual flipping of the competing percepts [6].

Computational and theoretical neuroscience accounts for multistability by assuming a mechanism of mutual inhibition among visually responsive neurons [9,10] (see also [4,5] for the case of decision making). These approaches imply the analysis of biophysically realistic neural circuits designed to implement stochastic transitions driven by noise. In general, these models involve populations of excitatory neurons engaged in competitive interactions mediated by inhibition. In this scenario the high and low activity states are stable for the same set of parameter values, i.e., the system is multistable. The computation involved in this type of processes is then understood as the fluctuation-driven, probabilistic transition between multistable states. If such circuits are comprised of large numbers of spiking neurons, the fluctuations needed to drive the transitions arise naturally through noisy input and/or disorder in the collective behavior of the network.

The temporal dynamics of the firing rates of the neuronal populations can be qualitatively captured via a system of first-order coupled differential equations of the Wilson-Cowan type [11,12] which describe the evolution of the average firing rate of each population. In this case, a fluctuation term must be added to drive the transitions, and one must study the corresponding Langevin equation of the firing-rate model. In order to capture the role of noise in a system of coupled differential equations, one option is to solve the associated Fokker-Planck equation for the probability distribution of the activities of the different neuronal populations. The nonlinear nature of the original equations, however, makes the analysis of the corresponding Fokker-Planck equation extremely cumbersome. For this reason, the main analysis of such noise-driven probabilistic systems remains based on time-consuming numerical investigations, because of the need for sufficiently many trials to capture the statistics of the data.

Tuckwell and Rodriguez ([13]; see also [14,15]) presented an alternative approach, called the method of moments (MM), which involves the derivation of deterministic differential equations for the first- and second-order moments of the distribution of the activity of the neuronal populations. (They applied this method in the context of the collective dynamics of coupled spiking neurons.) The resulting reduced system of deterministic equations lends itself to both analytical and numerical methods of solution as compared with the original Langevin equation. However, the application of the method of moments is restricted by the assumption that the distribution of the state variables of the system is a Gaussian.

*Also at Institució Catalana de Recerca i Estudis Avançats (ICREA), Barcelona, Spain. Electronic address: gustavo.deco@upf.edu

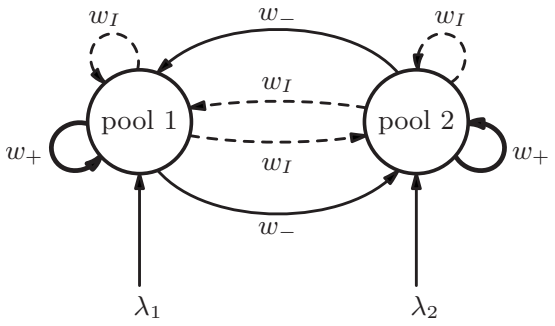

FIG. 1. Stochastic neurodynamical network consisting of two self- and mutually interacting neuronal populations. The activities of the specific populations may encode, for example, the two alternative percepts in the context of bistable perception phenomena. Continuous arrows represent excitatory connections between neurons in the same population with weight w_+ as well as between neurons in different populations with weight w_-. Dashed arrows represent inhibitory connections with weight w_I. External sensory input to the respective population is provided at rates λ_1 and λ_2.

In neuroscience, nevertheless, many interesting phenomena, like multistable perception or decision making, are naturally described by systems whose state variables (e.g., firing rates) are intrinsically bimodal. The aim of this paper is to extend the method of moments to the case of bimodal distribution of the state variables, such that a reduced system of deterministic coupled differential equations can be derived for the regime of multistability.

II. THEORY

Let us consider a canonical competitive network that contains two different populations of neurons. The activity of the neurons in each population encodes, for example, one of the two alternative percepts in a multistable context. The underlying connectivity is reflected in Fig. 1; we assume that the connections between neurons have already been formed according to Hebbian mechanisms, such that the coupling will be strong between neuron pairs with correlated activity and weak between pairs with uncorrelated activity. Accordingly, neurons within a specific population interact via strong recurrent excitation with a dimensionless weight $w_+ > 1$. On the other hand, since neurons in two different populations are likely to have anticorrelated activity in this behavioral context, we use a weaker excitatory weight $w_- < 1$ for the connections between them. Furthermore, we assume there is global feedback inhibition in the system, as a result of which all neurons are mutually coupled to all other neurons in an inhibitory way, with a weight denoted by w_I. The temporal dynamics of the firing rates of the neuronal populations is thus described by the following system of first-order differential equations [11,12]:

$$\tau \frac{d\nu_i(t)}{dt} = -\nu_i(t) + \phi\left(\lambda_i + \sum_{j=1}^{2} w_{ij}\nu_j(t)\right) + \sqrt{\tau}\xi_i(t), \quad (1)$$

where $\nu_i(t)$ denotes the firing rate of population $i=1,2$ at time t, w_{ij} is the synaptic strength between populations j and i (i.e., $w_{11}=w_{22}=w_+-w_I$ and $w_{12}=w_{21}=w_--w_I$), and τ is the time constant. The external, sensory input to the population i is denoted by λ_i, and the nonlinear transfer function $\phi(\cdot)$ is a sigmoid:

$$\phi(x) = \frac{\nu_{\max}}{1+\exp[-\alpha(x/\nu_c - 1)]}, \quad (2)$$

with saturation value $\nu_{\max}$ and maximal slope at ν_c. For simplicity we will assume that $\nu_{\max}=\nu_c$ and that $\alpha=4$ so that the maximal slope is 1. Fluctuations are modeled by adding independent Gaussian noise sources, denoted by ξ_i. Here $\langle \xi_i(t)\rangle = 0$ and $\langle \xi_i(t)\xi_j(t')\rangle = \beta^2\delta_{ij}\delta(t-t')$, where the angular brackets $\langle\cdot\rangle$ denote the average over realizations. This noise term represents finite-size effects that arise due to the finite number N of neurons in the populations (see [16,17]).

A standard bifurcation analysis of the fixed points can be performed for the noise-free case ($\beta=0$) corresponding to the limit $N\to\infty$, which leads to the so-called classical mean-field approximation [1,18,19]. For increasing w_+, the system undergoes a bifurcation. In particular, for values of w_+ higher than a certain critical value w_+^{crit}, the spontaneous activity state becomes unstable, and the system is forced to switch to either of the two remaining stable states, characterized by a high activation in one of the populations and low activation in the other. When noise is added to the system, and for $w_+ > w_+^{\text{crit}}$, the firing rates of the two populations have each a bimodal distribution, due to the transitions between the two stable states. Figure 2 shows a typical evolution of the firing rates (ν_1,ν_2) as a function of time. The system acts as a stochastic flip-flop circuit: the system remains in one of two possible stable states until fluctuations force it to switch to the other. Figure 3 shows the histograms for the firing rates, obtained by numerical integration of the system of stochastic differential equations (1).

In order to extend the method of moments to handle bimodal distributions of the state variables, we will derive a deterministic system of differential equations describing the moments of the state variables. Let us assume that the probability distribution of the state variables, here the firing rates ν_1 and ν_2 (we omit hereafter their explicit dependence on time), can be approximated by a bimodal Gaussian distribution given by

$$p(\nu_1,\nu_2) = Pg^{(1)}(\nu_1,\nu_2) + (1-P)g^{(2)}(\nu_1,\nu_2), \quad (3)$$

where $p(\nu_1,\nu_2)$ denotes the probability distribution of the state variables ν_i; $g^{(x)}(\nu_1,\nu_2)$ is a Gaussian distribution with mean value $\boldsymbol{\mu}^{(x)}=(\mu_1^{(x)},\mu_2^{(x)})$ and covariance matrix $\gamma_{ij}^{(x)}$; the superscript (x), where $x=1,2$, labels either of the two stable states present in the system. The variable P denotes the probability of being in the state $x=1$, i.e., in the bump described by the Gaussian distribution $g^{(1)}(\nu_1,\nu_2)$. Each Gaussian bump is described by five free parameters (the two components of the mean and three independent elements of the covariance matrix of the ν_i variables). Consequently, the bimodal distribution given by Eq. (3) is characterized by 11 parameters (five for each Gaussian bump, and the fraction P). These 11 parameters can also be extracted through 11 independent higher moments of the state variables

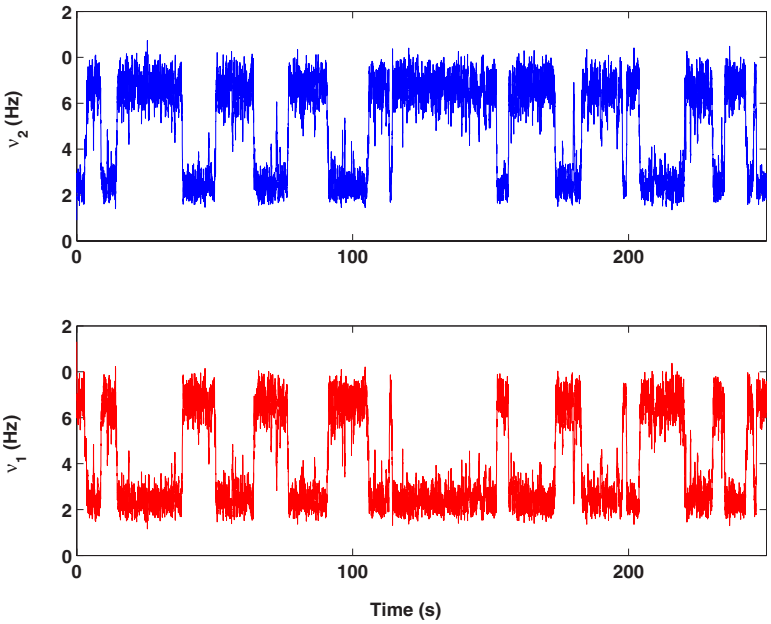

FIG. 2. (Color online) Temporal dynamics of the firing rates (ν_1, ν_2). The firing rates of both populations act as a stochastic flip-flop circuit, due to the stochastic transitions between the two bistable states.

(ν_1, ν_2).We define following first-, second-, third-, and fourth-order moments of the state variables:

$$\mu_i = \langle \nu_i \rangle = \sum_{x=1}^{2} P^{(x)} \mu_i^{(x)}, \tag{4}$$

$$\gamma_{ij} = \langle \delta\nu_i \delta\nu_j \rangle = \sum_{x=1}^{2} P^{(x)} (\gamma_{ij}^{(x)} + a_i^{(x)} a_j^{(x)}), \tag{5}$$

$$\Gamma_{ijk} = \langle \delta\nu_i \delta\nu_j \delta\nu_k \rangle = \sum_{x=1}^{2} P^{(x)} (\gamma_{ij}^{(x)} a_k^{(x)} + \gamma_{ik}^{(x)} a_j^{(x)} + \gamma_{jk}^{(x)} a_i^{(x)} + a_i^{(x)} a_j^{(x)} a_k^{(x)}), \tag{6}$$

$$\Phi_{iiii} = \langle (\delta\nu_i)^4 \rangle = \sum_{x=1}^{2} P^{(x)} [3(\gamma_{ii}^{(x)})^2 + 6\gamma_{ii}^{(x)} (a_i^{(x)})^2 + (a_i^{(x)})^4], \tag{7}$$

where we have defined $\delta\nu_i = \nu_i - \mu_i$, $P^{(1)} = P$, $P^{(2)} = 1 - P$, and $a_i^{(x)} = \mu_i^{(x)} - \mu_i$. Here, the angular brackets of $\langle f(\nu_1(t), \nu_2(t)) \rangle$ denote the average of an arbitrary function $f(\nu_1(t), \nu_2(t))$ defined by

$$\begin{aligned} \langle f(\nu_1, \nu_2) \rangle &= \int\int f(\nu_1, \nu_2) p(\nu_1, \nu_2) d\nu_1 d\nu_2 \\ &= P^{(1)} \langle f(\nu_1, \nu_2) \rangle_1 + P^{(2)} \langle f(\nu_1, \nu_2) \rangle_2 \\ &= P^{(1)} \int\int f(\nu_1, \nu_2) g^{(1)}(\nu_1, \nu_2) d\nu_1 d\nu_2 + P^{(2)} \\ &\quad \times \int\int f(\nu_1, \nu_2) g^{(2)}(\nu_1, \nu_2) d\nu_1 d\nu_2. \end{aligned} \tag{8}$$

Note that not all higher-order moments are independent (e.g., $\gamma_{12} = \gamma_{21}$); therefore, to select 11 independent parameters, one has to consider only moments that do not result from a permutation of the indices. One can expand Eq. (1) in a Taylor series about the mean values of the rate variables $\boldsymbol{\mu}$ yielding

$$\begin{aligned} \tau \frac{d\nu_i}{dt} &= -\nu_i + \sum_{n=0}^{\infty} \frac{1}{n!} \phi^{(n)}(u_i) \sum_{i_1=1}^{2} \cdots \sum_{i_n=1}^{2} w_{ii_1} \cdots w_{ii_n} \delta\nu_{i_1} \cdots \delta\nu_{i_n} + \sqrt{\tau}\xi_i \\ &= -\nu_i + \sum_{n=0}^{\infty} \frac{1}{n!} \phi^{(n)}(u_i) \sum_{m=0}^{n} \binom{n}{m} w_{i1}^m w_{i2}^{n-m} (\delta\nu_1)^m (\delta\nu_2)^{n-m} + \sqrt{\tau}\xi_i \end{aligned} \tag{9}$$

where $\phi^{(n)}(u_i)$ is the nth derivative of the function $\phi(x)$ applied at $u_i = \lambda_i + \Sigma_{j=1}^{2} w_{ij}\mu_j$. Averaging both sides, and taking into account that $\langle \delta\nu_i(t) \rangle = 0$, we obtain the following deterministic equations for the first-order moments:

$$\tau \frac{d\mu_i}{dt} = -\mu_i + \sum_{n=0}^{\infty} \frac{1}{n!} \phi^{(n)}(u_i) \sum_{m=0}^{n} \binom{n}{m} w_{i1}^m w_{i2}^{n-m} \Omega_{m,n-m} \tag{10}$$

where

$$\Omega_{m,n-m} = (P^{(1)} \Omega_{m,n-m}^{(1)} + P^{(2)} \Omega_{m,n-m}^{(2)}) \tag{11}$$

and

$$\Omega_{m,n-m}^{(x)} = \langle (\delta\nu_1)^m (\delta\nu_2)^{n-m} \rangle_x = \langle (\delta\nu_1^{(x)} + a_1^{(x)})^m (\delta\nu_2^{(x)} + a_2^{(x)})^{n-m} \rangle_x \tag{12}$$

with $\delta\nu_i^{(x)} = \nu_i - \mu_i^{(x)}$. Equation (12) can be written in a closed form by developing the binomial terms explicitly:

$$\Omega_{p,b}^{(x)} = \sum_{k=0}^{p} \sum_{j=0}^{b} \binom{p}{k} \binom{b}{j} [a_1^{(x)}]^{p-k} [a_2^{(x)}]^{b-j} \langle (\delta\nu_1)^k (\delta\nu_2)^j \rangle_x \tag{13}$$

and using the Isserlis [20] formula for the multivariate high-order moments of a Gaussian distribution:

$$\langle (\delta\nu_1)^k (\delta\nu_2)^j \rangle_x = \begin{cases} 0 & \text{if } k+j \text{ is odd,} \\ \gamma_{11}^k \gamma_{22}^j \dfrac{k!\, j!}{2^{s/2}} \displaystyle\sum_{r=0}^{t} \dfrac{(2\gamma_{12})^{2r}}{(k/2-r)!\,(j/2-r)!\,(2r)!} & \text{if } k \text{ and } j \text{ are even,} \\ \gamma_{11}^k \gamma_{22}^j \dfrac{k!\, j!}{2^{s/2}} \displaystyle\sum_{r=0}^{t} \dfrac{(2\gamma_{12})^{2r+1}}{[(k-1)/2-r]!\,[(j-1)/2-r]!\,(2r+1)!} & \text{if } k \text{ and } j \text{ are odd,} \end{cases} \tag{14}$$

where $t = \min(k,j)/2$. Similarly, since

$$\tau \frac{d\delta\nu_i}{dt} = -\nu_i + \sum_{n=0}^{\infty} \frac{1}{n!} \phi^{(n)}(u_i) \sum_{m=0}^{n} \binom{n}{m} w_{i1}^m w_{i2}^{n-m} \times [(\delta\nu_1)^m (\delta\nu_2)^{n-m} - \Omega_{m,n-m}] + \sqrt{\tau}\xi_i \tag{15}$$

holds, the deterministic equations for the higher-order moments can be derived by applying the chain rules in Eqs. (5)–(7) and using Eq. (15), yielding

$$\tau \frac{d\gamma_{11}}{dt} = -2\gamma_{11} + 2\sum_{n=0}^{\infty} \frac{1}{n!} \phi^{(n)}(u_1) \times \sum_{m=0}^{n} \binom{n}{m} w_{11}^m w_{12}^{n-m} \Omega_{m+1,n-m} + \beta^2, \tag{16}$$

$$\tau \frac{d\gamma_{22}}{dt} = -2\gamma_{22} + 2\sum_{n=0}^{\infty} \frac{1}{n!} \phi^{(n)}(u_2) \times \sum_{m=0}^{n} \binom{n}{m} w_{12}^m w_{22}^{n-m} \Omega_{m,n-m+1} + \beta^2, \tag{17}$$

$$\tau \frac{d\gamma_{12}}{dt} = -2\gamma_{12} + \sum_{n=0}^{\infty} \frac{1}{n!} \sum_{m=0}^{n} \binom{n}{m} [\phi^{(n)}(u_1) w_{11}^m w_{12}^{n-m} \Omega_{m,n-m+1} + \phi^{(n)}(u_2) w_{12}^m w_{22}^{n-m} \Omega_{m+1,n-m}], \tag{18}$$

$$\tau \frac{d\Gamma_{111}}{dt} = -3\Gamma_{111} + 3\sum_{n=0}^{\infty} \frac{1}{n!} \phi^{(n)}(u_1) \times \sum_{m=0}^{n} \binom{n}{m} w_{11}^m w_{12}^{n-m} (\Omega_{m+2,n-m} - \gamma_{11}\Omega_{m,n-m}), \tag{19}$$

$$\tau \frac{d\Gamma_{112}}{dt} = -3\Gamma_{112} + \sum_{n=0}^{\infty} \frac{1}{n!} \sum_{m=0}^{n} \binom{n}{m} [2\phi^{(n)}(u_1) w_{11}^m w_{12}^{n-m} \times (\Omega_{m+1,n-m+1} - \gamma_{12}\Omega_{m,n-m}) + \phi^{(n)}(u_2) w_{12}^m w_{22}^{n-m} \times (\Omega_{m+2,n-m} - \gamma_{11}\Omega_{m,n-m})], \tag{20}$$

$$\tau \frac{d\Gamma_{122}}{dt} = -3\Gamma_{122} + \sum_{n=0}^{\infty} \frac{1}{n!} \sum_{m=0}^{n} \binom{n}{m} [\phi^{(n)}(u_1) w_{11}^m w_{12}^{n-m} \times (\Omega_{m,n-m+2} - \gamma_{22}\Omega_{m,n-m}) + 2\phi^{(n)}(u_2) w_{12}^m w_{22}^{n-m} \times (\Omega_{m+1,n-m+1} - \gamma_{12}\Omega_{m,n-m})], \tag{21}$$

$$\tau \frac{d\Gamma_{222}}{dt} = -3\Gamma_{222} + 3\sum_{n=0}^{\infty} \frac{1}{n!} \phi^{(n)} \times (u_2) \sum_{m=0}^{n} \binom{n}{m} w_{12}^m w_{22}^{n-m} (\Omega_{m,n-m+2} - \gamma_{22}\Omega_{m,n-m}), \tag{22}$$

$$\tau \frac{d\Phi_{1111}}{dt} = -4\Phi_{1111} + 4\sum_{n=0}^{\infty} \frac{1}{n!} \phi^{(n)}(u_1) \sum_{m=0}^{n} \binom{n}{m} w_{11}^m w_{12}^{n-m} \times (\Omega_{m+3,n-m} - \Gamma_{111}\Omega_{m,n-m}) + 6\gamma_{11}\beta^2, \tag{23}$$

$$\tau \frac{d\Phi_{2222}}{dt} = -4\Phi_{2222} + 4\sum_{n=0}^{\infty} \frac{1}{n!} \phi^{(n)}(u_2) \sum_{m=0}^{n} \binom{n}{m} w_{12}^m w_{22}^{n-m} \times (\Omega_{m,n-m+3} - \Gamma_{222}\Omega_{m,n-m}) + 6\gamma_{22}\beta^2. \tag{24}$$

The noise term in Eqs. (16), (17), (23), and (24) was derived according to Itō calculus. In Itō calculus, white noise $\xi(t)$ is seen as the time derivative of a Wiener process or Brownian motion $W(t)$, i.e., $dW(t) = \xi(t)dt$. Our equations have the stochastic differential form $dX = Fdt + G\,dW$, with $G = \beta\sqrt{\tau}$, and we can apply Itō's chain rule to obtain the differential form

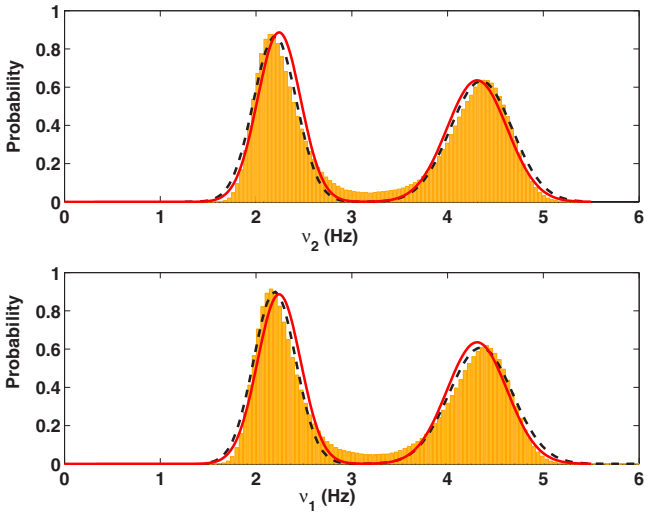

FIG. 3. (Color online) Probability density functions of the stationary asymptotic distributions of ν_1 (lower panel) and ν_2 (top panel) for $\beta=0.0632$ Hz, $w_+=2.32$, and $\Delta\lambda=0$ (unbiased case). Using (1) we integrated a single trial during 1000 ss. Mean values of the firing rates calculated from nonoverlapping intervals of 1 ms were used to construct normalized histograms (orange shaded areas). Gaussian bumps with means and variances given by solutions of the reduced deterministic moments systems [Eqs. (10) and (16)–(24) are shown as red solid curves. The best (in the sense of maximum likelihood) fits of the simulated data using Eq. (1) obtained with a bimodal Gaussian model are shown as dashed black curves.

of any power of X; following Itō's rule, the stochastic differential form for $Y \equiv X^m$ is

$$dY = \left[mX^{m-1}F + \tfrac{1}{2}m(m-1)X^{m-2}G^2\right]dt + mX^{m-1}G\,dW,$$

where the unexpected term (according to conventional calculus) $\frac{1}{2}m(m-1)X^{m-2}G^2dt$ arises from the fact that $dW \sim \sqrt{dt}$.

Hence, the original system described by the two Langevin equations (1) is transformed into a system of 11 coupled deterministic differential equations relating the higher-order moments of the probability distributions of the rates ν_1 and ν_2. Solving the fixed points of the deterministic system of moments by setting the left-hand side of Eqs. (10) and (16)–(24) equal to zero allows us to find the 11 parameters P, $\mu_i^{(x)}$, and $\gamma_{ij}^{(x)}$ (for all i and x) that characterize the assumed bimodal Gaussian distribution of the state variables, avoiding explicit trial-by-trial simulations of the original Langevin system. We solve this system numerically by applying a nonlinear least-square solver based on the Levenberg-Marquardt method with line search [21] and truncating the infinite summation on the right-hand side of Eqs. (10) and (16)–(24) at a finite $n=N$. In the numerical experiments, we assessed the convergence of the truncated summation by increasing successively the value of N and checking that the terms with increasing n were becoming negligible. Note that one can calculate the derivative $\phi^{(n)}$ iteratively using the following expression:

$$\phi^{(n)} = \frac{\alpha}{\nu_c}\phi^{(n-1)} - 2\frac{\alpha}{\nu_c \nu_{\max}}\sum_{j=0}^{n-2} a_{n,j}\phi^{(j)}\phi^{(n-j-1)} \quad \text{for } n \geq 2 \tag{25}$$

where

$$a_{n,j} = \begin{cases} 1 & \text{if } j = 0 \text{ or } j = n-2, \\ a_{n,j} = a_{n-1,j-1} + a_{n-1,j} & \text{otherwise.} \end{cases} \tag{26}$$

III. RESULTS

We show in this section the application of the extended MM to the multistable neurodynamical system introduced in the last section and described by Eq. (1). The explicit numerical simulations of the neurodynamical system (1) reflecting the effect of stochastic fluctuations on that system can now be compared with the semianalytical results obtained by the reduced deterministic moments systems [Eqs. (10) and (16)–(24)]. In all experiments, we truncated the right-hand side of Eqs. (10) and (16)–(24) at $N=10$, after checking convergence.

The parameter values used in the simulations were $\tau=1$ ms, $\lambda_1=15$ Hz, and $\lambda_2=\lambda_1+\Delta\lambda$, where $\Delta\lambda$ is varied from 0 to 6 μHz. We selected the parameters in order that the system be bistable.

Figure 3 plots the probability density functions of the stationary asymptotic distributions of ν_1 (lower panel) and ν_2 (top panel) for $\beta=0.0632$ Hz, $w_+=2.32$, and $\Delta\lambda=0$ (unbiased case). The explicit numerical simulations of the original Langevin system (1) were obtained by integrating a single trial during 1000 s. We integrated numerically Eqs. (1) with the Euler method by discretizing them in the following way:

$$\nu_i(t+\Delta t) = \nu_i(t) + \frac{\Delta t}{\tau}\left[-\nu_i(t) + \phi\left(\lambda_i + \sum_{j=1}^{2} w_{ij}\nu_j(t)\right)\right] + \beta\psi_i\sqrt{\frac{\Delta t}{\tau}}, \quad i=1,2,$$

$$+ \beta\psi_i\sqrt{\frac{\Delta t}{\tau}}, \quad i=1,2, \tag{27}$$

where ψ_i are independent standard normalized Gaussian noise processes. Mean values of the firing rates calculated from nonoverlapping intervals of 1 ms were used to construct the normalized histograms [(shaded) orange areas in Fig. 3]. Solutions for the stationary bimodal Gaussian distributions with parameters (mean values, covariances, and weighting factor P) obtained by the extended deterministic system of moments [Eqs. (10) and (16)–(24)] are shown as (red) solid curves in Fig. 3. They agree well with the numerical solutions of the original Langevin equations. Even more, for comparison, Fig. 3 also depicts a bimodal Gaussian maximum-likelihood fit (dashed black curves) of the simulated data using Eq. (1), which shows as well a good agreement with the results obtained by the extended MM.

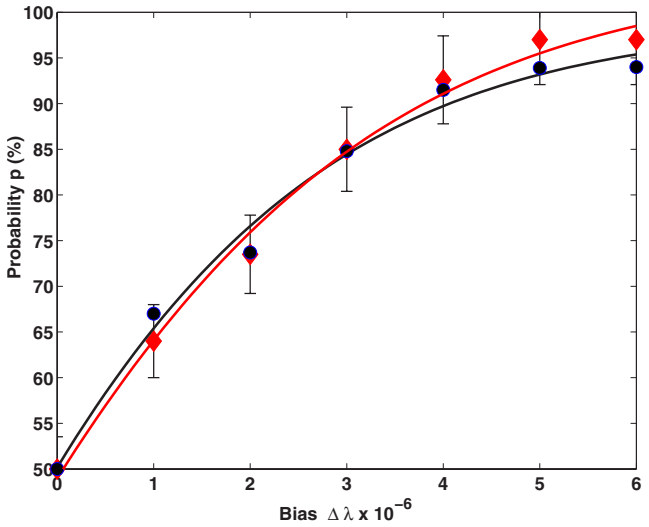

FIG. 4. (Color online) Probability P of being in one of the bistable state ($x=1$) as a function of the external bias $\Delta\lambda$. Red (gray) diamonds: Explicit numerical simulation using Eq. (1) (single trial during 1000 simulated seconds). Black circles: Reduced deterministic moments method [fixed points of Eqs. (10) and (16)–(24)]. The red (gray) and black lines are Weibull fitting curves corresponding to the explicit numerical simulations [red (gray) diamonds] and the moment method (black circles).

We have also obtained an excellent numerical agreement for the moments $\mu_i^{(x)}$ and $\gamma_{ij}^{(x)}$ between those estimated by the MM and those estimated by the maximum-likelihood (ML) estimators obtained from the simulated data. For example, the two estimates (ML and MM, the latter in parentheses) for the different moments of ν_1 (top panel of Fig. 3) are $\mu_1^{(1)}=2.19$ (2.2), $\mu_1^{(2)}=4.35$ (4.3), $\gamma_{11}^{(1)}=0.0505$ (0.0506), $\gamma_{11}^{(2)}=0.1046$ (0.0985). To study the more general biased case ($\Delta\lambda\neq 0$), we analyze the dependence of the main variable P (probability of being in one of the two bistable states, namely, the state $x=1$) as a function of the bias $\Delta\lambda$. Figure 4 plots the numerical results obtained by explicit simulations of the original system (red diamonds) and the results obtained by the reduced deterministic moments method (black circles). To facilitate visualisation, we added Weibull fitting curves, traditionally used in the psychophysical literature. These results show a very good agreement between numerical simulations and the extended moments method.

The influence of the bias results in an increase of the probability of permanence in one of the two bumps of the bimodal distribution, namely, in the one corresponding to a high activation of the neuronal population receiving the external bias and low activation in the other neuronal population. For the particular case of $\Delta\lambda=0$ (unbiased case), $P=0.5$, i.e., the system is 50% of the time in each bump. On the other hand, for high enough $\Delta\lambda$ the system is most of the time in the state (bump) corresponding to the high activation of the externally biased neuronal population. Note that the increasing difference between the MM results and the simulations for increasing $\Delta\lambda$ is probably due to the fact that the explicit numerical integration of the original Langevin system (1) requires longer simulations.

IV. DISCUSSION

In this paper we extended the moments method to the case of bimodal distributions of the state variables (e.g., firing rates, in a neurodynamical context), such that a reduced system of deterministic differential equations characterizing the parameters of the bimodal distribution can be derived for the regime of multistability. This extension is relevant for computational neuroscience, because many perceptual and cognitive functions involve multistable phenomena. In a multistable regime, noise appears as a decisive parameter whose tuning determines the capability of the system to perform decision making or multistable perception. Therefore, the aim of this work is to present a method that allows us to investigate the role of stochastic fluctuations in a system of differential equations describing the underlying neurodynamics. Traditionally, one approach to this problem has been to solve the associated Fokker-Planck equation for the probability distribution of the activities of the different neuronal populations. The nonlinear nature of the original neurodynamical equations hinders analytical progress in the Fokker-Planck framework. On the other hand, numerical investigations are time consuming since they require a large set of trials or long simulations to generate statistically meaningful data. The moments method offers an alternative approach that involves the derivation of deterministic differential equations for the higher-order moments of the distribution of the activity of the neuronal populations. The resulting reduced system of deterministic equations lends itself to both analytical and numerical methods of solutions as compared with the original Langevin equation.

ACKNOWLEDGMENTS

This work was supported by the European Union, Grant No. EC005-024 (STREP "Decisions in Motion") and by the Spanish Research Project No. TIN2004-04363-C03-01. G.D. was supported by Institució Catalana de Recerca i Estudis Avançats (ICREA).

[1] H. C. Tuckwell, *Introduction to Theoretical Neurobiology* (Cambridge University Press, Cambridge, U.K., 1988).
[2] E. T. Rolls and G. Deco, *Computational Neuroscience of Vision* (Oxford University Press, Oxford, 2002).
[3] C. Brody, R. Romo, and A. Kepecs, Curr. Opin. Neurobiol. **13**, 204 (2003).
[4] C. Machens, R. Romo, and C. Brody, Science **307**, 1121 (2005).
[5] G. Deco and E. Rolls, Eur. J. Neurosci. **24**, 901 (2006).
[6] D. Leopold and N. Logothetis, Trends Cogn. Sci. **3**, 254 (1999).
[7] F. Attneave, Sci. Am. **225**, 63 (1971).

[8] M. Taylor and K. Aldridge, Percept. Psychophys. **16**, 9 (1974).
[9] C. Laing and C. Chow, J. Comput. Neurosci. **12**, 39 (2002).
[10] H. Wilson, Proc. Natl. Acad. Sci. U.S.A. **100**, 14499 (2003).
[11] A. Renart, N. Brunel, and X. Wang, in *Computational Neuroscience: A Comprehensive Approach*, edited by J. Feng (Chapman and Hall, Boca Raton, FL, 2003), pp. 431–490.
[12] G. La Camera, A. Rauch, H. Luescher, W. Senn, and S. Fusi, Neural Comput. **16**, 2101 (2004).
[13] R. Rodriguez and H. C. Tuckwell, Phys. Rev. E **54**, 5585 (1996).
[14] R. Rodriguez and H. C. Tuckwell, BioSystems **48**, 187 (1998a).
[15] H. C. Tuckwell and R. Rodriguez, J. Comput. Neurosci. **5**, 91 (1998).
[16] M. Mattia and P. Del Giudice, Phys. Rev. E **70**, 052903 (2004).
[17] M. Mattia and P. Del Giudice, Phys. Rev. E **66**, 051917 (2002).
[18] N. Brunel and X. Wang, J. Comput. Neurosci. **11**, 63 (2001).
[19] D. Amit and N. Brunel, Cereb. Cortex **7**, 237 (1997).
[20] L. Isserlis, Biometrika **12**, 134 (1918).
[21] J. More, in *Numerical Analysis*, edited by G. Watson, Lecture Notes in Mathematics, Vol. 630 (Springer-Verlag, Berlin, 1977), pp. 105–116.